arXiv:1603.04920v1 [math.NA] 15 Mar 2016

TEMPORAL UPSCALING IN MICRO MAGNETISM VIA HETEROGENEOUS MULTISCALE METHODS

DOGHONAY ARJMAND, STEFAN ENGBLOM, AND GUNILLA KREISS

Abstract. We consider a multiscale strategy addressing the disparate temporal scales in the Landau-Lifschitz equations of micro-magnetism. At the microscopic scale, the magnetisation dynamics is driven by either a high frequency field when considering ferromagnetic resonance, or a white noise process modeling thermal fluctuations. On the macroscopic scale we are interested in simulating the dynamics of single magnetic spins without fully resolving the microscopic scales.

The method follows the framework of heterogeneous multiscale methods and it has two main ingredients: a micro- and a macroscale model. The microscopic model is assumed to be known exactly whereas the macro model is incomplete as it lacks effective parameter values. The two models are integrated at different temporal resolution and effective parameter values for the macro model are computed on the fly, allowing for improved efficiency over traditional one-scale schemes.

For the analysis, we consider a deterministic high frequency field and show that effective parameter values can be obtained accurately with step-sizes much larger than the size of the microscopic scales required to resolve the microscopic scale. We consider also the stochastic setting and verify via numerical experiments that the effective dynamics are accurately captured.

1. Introduction

Suppose that we are given an ensemble of particles $\{i\}_{i=1}^N$, each of them possessing a magnetisation represented by $\mathbf{m}_i(t) \in \mathbb{R}^3$, for all $t \in [0,T]$. At a microscopic level, the dynamics of the magnetisation of the particle i is modeled by the Landau-Lifschitz (LL) equation, [26]:

$$\partial_t \mathbf{m}_i = \beta \mathbf{m}_i \times \mathbf{H}_i - \gamma \mathbf{m}_i \times (\mathbf{m}_i \times \mathbf{H}_i)\,. \tag{1.1}$$

The first term on the right hand side accounts for the precessional motion of the magnetisation $\mathbf{m}_i$ around a field $\mathbf{H}_i$ while the nonlinear term is responsible for damping the magnetisation toward the field $\mathbf{H}_i$. In general, the effective field $\mathbf{H}_i$ accounts for the contributions of different short and long range interactions. In the presence of exchange, anisotropy, and an external field, $\mathbf{H}_i$ is given by

$$\mathbf{H}_i = \sum_j J_{ij}\mathbf{m}_j + K_{ani}\mathbf{p}\cdot\mathbf{m}_i + \tilde{\mathbf{H}},$$

where J_{ij} is the exchange rate between the particles i and j, $\mathbf{p}$ is the material anisotropy which is the energetically favourable direction of magnetisation, and where $\tilde{\mathbf{H}}$ is an external field interacting with the particles. Note that the above

2010 *Mathematics Subject Classification.* Primary: 65L04; Secondary: 65L05, 65L70.

Key words and phrases. Micro magnetism, Landau-Liftshitz equations, Heterogeneous multiscale methods.

form of $\mathbf{H}_i$ is stated only for a general introduction of the LL equation and to illustrate the idea behind multiscale methods. However, the theoretical settings in this paper will cover the contribution of the external field $\tilde{\mathbf{H}}$ only.

We are often interested in the dynamics of the magnetisation at scales much larger than the size of the spatial and temporal variations at a particle level. It is, however, computationally unaffordable to solve the microscopic model over the entire domain to simulate *macroscopic dynamics* of the magnetisation process. The macroscopic quantities can be defined as e.g. local averages, in time and space, of the magnetisations of the particles. A traditional approach is the molecular field approximation, where an equation for the volume-averaged magnetisation is derived [2]. Such an approach, however, lacks generality as the approximation may not be valid e.g. in the vicinity of microscopic defects. To treat microscopic irregularities, it is therefore necessary to develop multiscale strategies that can iterate back and forth between an accurate microscopic and a computationally efficient macroscopic model. The microscopic model is expensive and, therefore, should be used only when necessary.

There are two common types of multiscale strategies to couple the disparate scales in multiscale problems. The first approach is the domain partitioning strategy which implies an explicit interface between mathematical laws valid at different scales. The other alternative is to use methods based on upscaling, where a macroscopic model is assumed everywhere and the microscopic information is upscaled to the macro model only in a small part of the domain when, for example, the molecular field approximation breaks down and a more detailed description is needed. Schematics of these approaches are given in Figure 1.1. There are a large number of related literature on coupling different length scales in magnetism. Without being exhaustive we refer the curious reader to [8, 12, 13, 16, 23, 30, 33].

In this article, as a first step towards designing general multiscale methods such as the upscaling strategy illustrated in Figure 1.1 (the left schematic), we propose and analyse an upscaling strategy based on heterogeneous multiscale methods (HMM) [18], to couple disparate temporal scales in the LL equations. The algorithm assumes a macro model where some data in the model are missing. These data are then computed and upscaled by carrying out simulations in localised, in time, microscopic domains. As we limit ourselves to the analysis of temporal upscaling only, we consider a model problem where the effective field $\mathbf{H}$ includes the influence of a time-dependent external field with no particle interactions. Since we do not have any interaction, such as exchange, among the particles, we regard all particles as being identical and rewrite the LL equation (1.1) as

$$\partial_t \mathbf{m}^\varepsilon = \beta \mathbf{m}^\varepsilon \times \mathbf{H}^\varepsilon - \gamma \mathbf{m}^\varepsilon \times (\mathbf{m}^\varepsilon \times \mathbf{H}^\varepsilon)\,. \tag{1.2}$$

In this setting the magnetisation dynamics of a particle is driven only by an external field $\mathbf{H}^\varepsilon$, which may possess slow and fast variations at the same time. The parameter $\varepsilon \ll 1$ denotes the wave-length of the rapid variations. The high-frequency component of $\mathbf{H}^\varepsilon$ may be a deterministic term, as in ferromagnetic resonance (FMR), see [24], or a random field which is used in the modeling of temperature effects in micro-magnetism, [11]. The external field is usually written in the form $\mathbf{H}^\varepsilon(t) := \mathbf{H}_0(t) + \mathbf{H}_1^\varepsilon(t)$, where $\mathbf{H}_0$ is a smooth field, typically a constant state, and $\mathbf{H}_1^\varepsilon$ is a high frequency component which fluctuates with the wavelength $\varepsilon \ll 1$. We are mainly interested in two settings:

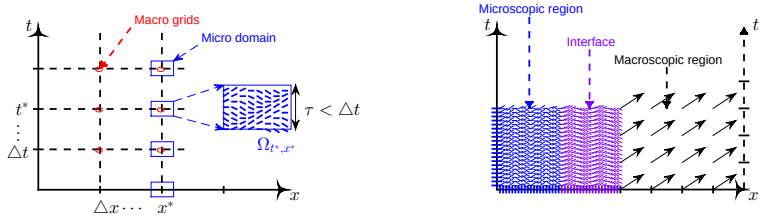

FIGURE 1.1. (Left) A multiscale strategy based on upscaling: The macroscopic model lacks some information in the center of the micro boxes, e.g. at (t^*, x^*). The missing effective parameter values are then computed by carrying out local, in time and space, microscopic simulations in small boxes, e.g. Ω_{t^*,x^*}. The micro problems should be synchronised with the corresponding coarse scale data and the effective quantities are computed and upscaled from the micro to the macro level. (Right) A multiscale strategy based on domain partitioning: Different mathematical laws are valid at different regions. The macroscopic region does not see the small scale variations in the microscopic domain. These two regions are connected by an interface. The interface acts as a transition region and conditions are often imposed to ensure the consistency between the microscopic and the macroscopic quantities.

1. $\mathbf{H}^\varepsilon = \mathbf{H}_0(t) + \mathbf{H}_{det}(t/\varepsilon)$
2. $\mathbf{H}^\varepsilon = \mathbf{H}_0(t) + \mathbf{H}^\varepsilon_{sto}(t)$,

modeling deterministic and stochastic fluctuations, respectively. We will carry out the analysis for the deterministic case, but we provide numerical results showing the applicability of the method to the stochastic setting as well. In the stochastic framework, the upscaling algorithm we introduce in this paper can be seen as an alternative to the well-known Landau-Lifshitz-Bloch (LLB) equations, derived in [22], which approximate the macroscopic dynamics of stochastic Landau-Lifshitz (SLL) equations, see also [9, 8] for an LLB-type macroscopic model valid at high temperatures. More detailed discussion about this can be found in Section 3.3. Although the theoretical findings in the current study do not cover the full LL equations with all energy terms, they present a good insight regarding the sources of errors in a typical multiscale coupling based on upscaling. For the analysis in the deterministic setting, we assume that $\mathbf{H}^\varepsilon(t) = \mathbf{H}(t, t/\varepsilon)$ so that $\mathbf{m}^\varepsilon$ has non-trivial dependence on the slow and fast scales, which is a better representative of the situation when other energy contributions are taken into account.

Remark 1. *Note that there are two variants of SLL equations in the literature. The first variant, see e.g. [32], considers the noise both in the precession and the damping term, as in equation (1.2), while in the second variant, [8], the noise term is included only in the precessional term. The numerical method here is developed for the former. Note also that in the stochastic setting, the SLL equation (1.2) should be interpreted in the Stratonovic sense.*

The paper is structured as follows. In Section 2, we introduce the notation and preliminary results which will be used later in the analysis. In Section 3, we give a general overview of HMM for multiscale ordinary differential equations (ODEs) and we also present our multiscale algorithm. Section 4 is devoted to the analysis of the method where a fully discrete estimate for the difference between the HMM solution and the exact local average is given. Finally, we conclude our paper by presenting numerical examples corroborating our theoretical statements.

2. Preliminaries

2.1. **Notation.** We will use calligraphic fonts, e.g. $\mathcal{H}(t)$, to denote matrices or matrix functions. Vector functions are represented by a bold face letter, e.g. $\mathbf{m}(t)$. Macroscopic and microscopic step-sizes will be denoted by $\triangle t$ and δt, respectively. The space of functions of bounded variations is written as $BV(\mathbb{R})$. The Euclidian 2-norm is written as $|\mathbf{m}|_2 = \sqrt{m_1^2 + m_2^2 + m_3^2}$ and we denote the corresponding inner-product by $\langle \mathbf{u}, \mathbf{v} \rangle = \sum_{i=1}^{d} \mathbf{u}_i \mathbf{v}_i$. Unless otherwise specified, $|\cdot|$ is to mean $|\cdot|_2$. Throughout the paper, the constant $C = O(1)$ is a generic constant whose value may change in subsequent occurences.

2.2. **Utility results.** The upscaling strategy that is summarised in the next section is heavily based on the notion of local averages. Assume that we have an oscillatory function $f^\varepsilon(t) := f(t/\varepsilon)$ for $t \in [0, T]$, where f is a 1-periodic function and $\varepsilon \ll 1$. The function $f(t/\varepsilon)$ is then ε-periodic. To compute the local average we introduce an interval $I_\tau := [-\tau/2, \tau/2]$, where $\tau = O(\varepsilon)$. A naive local averaging approach is to integrate the function f^ε over the interval I_τ. The following estimate for the error of this naive averaging can easily be shown.

$$\left| \frac{1}{\tau} \int_{-\tau/2}^{\tau/2} f(s/\varepsilon)\, ds - \int_0^1 f(s) ds \right| \leq C \frac{\varepsilon}{\tau}. \tag{2.1}$$

In this paper, τ stands for the size of the microscopic simulations and it should practically be chosen of the same order as ε. But the error in (2.1) can be very large when $\tau = O(\varepsilon)$. To reduce this error, we introduce the space of kernels $\mathbb{K}^{p,q}$ and we say that $K \in \mathbb{K}^{p,q}$ if K has a compact support in $[-1/2, 1/2]$ and

- $K(t) = K(-t)$
- $K^{(q+1)} \in BV(\mathbb{R})$
- K has p vanishing moments:

$$\int_{\mathbb{R}} K(t) t^r dt = \begin{cases} 1 & r = 0, \\ 0, & 0 < r \leq p. \end{cases}$$

Note that $K^{(q+1)}$ is the $(q+1)th$ weak derivative and that a constant kernel belongs to $K^{1,-1}$. To localise the kernel we introduce a scaled version $K_\tau(t) := 1/\tau K(t/\tau)$, with $K \in \mathbb{K}^{p,q}$. The local averages can then be computed by taking a weighted average of the function f^ε with K_τ over the domain I_τ. The following lemma from [6] shows how the convergence rate in (2.1) improves upon using such averaging kernels.

Lemma 1 (Lemma 2.3 in [6]). *Let f be a 1-periodic bounded function such that $f \in L^\infty([0,1])$ and $K \in \mathbb{K}^{p,q}$. Then with $\bar{f} = \int_0^1 f(s)ds$ we have*

$$\left| \int_{-\tau/2}^{\tau/2} K_\tau(s) f(s/\varepsilon)\, ds - \bar{f} \right| \leq C\, |f|_\infty \left(\frac{\varepsilon}{\tau}\right)^{q+2},$$

where the constant $C > 0$ is independent of ε and τ but may depend on K, f, p or q.

Remark 2. *Note that, in its original form in [6], the Lemma 1 assumes continuity of the integrand f. However, if the derivatives are interpreted in the weak sense, the same proof will be valid under the condition that $f \in L^\infty([0,1])$, see Figure 2 in [7] for a numerical verification of this statement.*

A well-known property of the LL equation (1.1) is the conservation of the length of magnetisation. In other words, if $|\mathbf{m}(0)|_2 = 1$, the magnetisation vector $\mathbf{m}(t)$ will stay on the unit sphere $\mathbb{S}^2$ in $\mathbb{R}^3$ for all $t \in [0,T]$. This can be seen by taking the inner-product of (1.1) by $\mathbf{m}(t)$. From a numerical point of view, it is then desirable to use discretisation schemes that respect this property. We refer to [14] for a survey of common time stepping schemes for the LL equation, to [31] for an analytical treatment of general computational approaches and to [25] for the treatment of relaxation based models used in stationary micromagnetism. One commonly used time-stepping scheme that preserves the magnetisation amplitude along with other invariants such as the Hamiltonian and the Lyapunov structures is the midpoint rule, see [15] for the analysis of the midpoint rule and [28] for a variant of it. The midpoint rule for (1.1) is

$$\mathbf{m}_{n+1} = \mathbf{m}_n + \beta \triangle t \mathbf{m}_{n+1/2} \times \mathbf{H}_{n+1/2} - \gamma \triangle t \mathbf{m}_{n+1/2} \times \left(\mathbf{m}_{n+1/2} \times \mathbf{H}_{n+1/2}\right),$$

where $\mathbf{u}_{n+1/2} = (\mathbf{u}_n + \mathbf{u}_{n+1})/2$ for $\mathbf{u} = \mathbf{m}$ or $\mathbf{u} = \mathbf{H}$. In this paper, we will use the mid-point rule as our choice of temporal discretisation for the LL equation. However, we emphasise that the multiscale method that we describe in the next section can easily be modified for any integration method with no conceptual change in the coupling conditions.

Finally, we state a simple inequality that is used in the proof of Lemma 3 below.

Lemma 2. *Suppose that the relation*

$$\frac{1}{2}\frac{d}{dt}\psi^2(t) \leq f(t)\psi(t)$$

holds for sufficiently smooth $\psi > 0$. Then we have the obvious inequality

$$\psi(T) \leq \psi(0) + \int_0^T f(s)ds. \tag{2.2}$$

3. The multiscale method

3.1. **Heterogeneous multiscale methods.** HMM was originally proposed by E and Engquist [18] as a general framework for designing multiscale algorithms for coupling mathematical models at different scales. For a recent account of applications of HMM in various fields, see the survey article [1]. Here we refer to [21, 4, 5, 3, 17] for the analysis and developments in the context of ordinary differential equations (ODEs) with multiple scales. For the analysis of HMM in the stochastic setting, see e.g. [34, 19]. Before proceeding further to the presentation

of our multiscale method, we present the general idea behind HMM. For this, we introduce

$$(\mathcal{K}\mathbf{m}^\varepsilon)(t_a) := \int K_\tau(t-t_a)\mathbf{m}^\varepsilon(t)\,dt.$$

We can then see that $\mathcal{K}\partial_t = \partial_t\mathcal{K}$. Next, we apply the operator $\mathcal{K}$ to both sides of the equation (1.2) and use the commutative property to see that, with $\mathbf{M}(t) := (\mathcal{K}\mathbf{m}^\varepsilon)(t)$,

$$\partial_t\mathbf{M}(t) = \beta\left(\mathcal{K}\left(\mathbf{m}^\varepsilon\times\mathbf{H}^\varepsilon\right)\right)(t) - \gamma\left(\mathcal{K}\left(\mathbf{m}^\varepsilon\times\left(\mathbf{m}^\varepsilon\times\mathbf{H}^\varepsilon\right)\right)\right)(t).$$

The macro variable $\mathbf{M}$ is smooth since by definition the fluctuations in $\mathbf{m}^\varepsilon$ are filtered out. Moreover, the right hand side $\partial_t\mathbf{M}$ is given by a local average of the original LL which oscillates around and damps towards the external field $\mathbf{H}^\varepsilon$. This suggests that we may assume a macro solver of the form:

$$\partial_t\mathbf{M}(t) = \mathbf{F}(t,\mathbf{M}), \tag{3.1}$$

where $\mathbf{F}$ is given by solving the original LL only locally and averaging the time derivative $\partial_t\mathbf{m}^\varepsilon$. In the next section, we propose a strategy which is different than a typical HMM in two respects: (i) We do not consider the above-mentioned form for the macro-solver, (ii) While computing the effective parameter, e.g. $\mathbf{F}$ in the above case, which requires solving the LL equation (1.2) locally, we will not include the damping term. We will show later, by analytical and numerical means, that this strategy does not induce any additional error.

3.2. **HMM for the LL equation (1.2) with deterministic $\mathbf{H}^\varepsilon$.** The effective equation on the macro level assumes the following form:

$$\text{Macro Model: } \begin{cases} \partial_t\mathbf{M}(t) = \mathbf{F}(t,\mathbf{M}) - \dfrac{\gamma}{\beta}\mathbf{M}\times\mathbf{F}(t,\mathbf{M}), \quad t\in(0,T], \\ \mathbf{M}(0) = \mathbf{m}^\varepsilon(0), \end{cases} \tag{3.2}$$

where $\mathbf{F}$ is the missing data in the model. Note that, unlike the model (3.1), the macro model (3.2) includes also a damping term . As the macro-solver, we use the midpoint rule due to the mentioned conservation properties it possesses. In principle, the HMM introduced in this section can be combined with any time-stepping scheme with no change in the macroscopic and microscopic models. In this paper, we will carry out the analysis for the implicit midpoint rule. The macro-solver uses a macro step-size $\triangle t$ and reads as

$$\text{Macro Solver: } \begin{cases} \mathbf{M}_{n+1} = \mathbf{M}_n + \triangle t\mathbf{F}_{n+1/2} - \dfrac{\gamma}{\beta}\triangle t\mathbf{M}_{n+1/2}\times\mathbf{F}_{n+1/2}, \\ \mathbf{M}_0 = \mathbf{m}^\varepsilon(0), \end{cases} \tag{3.3}$$

where $\mathbf{F}_{n+1/2} := \mathbf{F}\left(t_{n+1/2},\mathbf{M}_{n+1/2}\right)$, $t_{n+1/2} := (t_n+t_{n+1})/2$ and $\mathbf{M}_{n+1/2} = (\mathbf{M}_n + \mathbf{M}_{n+1})/2$. To close the system one needs to compute the right hand side $\mathbf{F}(t_a,\mathbf{M})$. To achieve this we first solve the micro model:

$$\text{Micro Model: } \begin{array}{l} \partial_t\mathbf{m}^\varepsilon(t) = \beta\mathbf{m}^\varepsilon(t)\times\mathbf{H}^\varepsilon(t), \quad t\in I_\tau^\pm, \\ \mathbf{m}^\varepsilon(t_a) = \mathbf{M}, \end{array} \tag{3.4}$$

where $I_\tau^+ := (t_a, t_a+\tau/2]$ and $I_\tau^- := [-\tau/2+t_a, t_a)$. Then, $\mathbf{F}(t_a,\mathbf{M})$ can be computed by:

$$\text{Upscaling: } \mathbf{F}(t_a,M) = (\mathcal{K}\partial_t\mathbf{m}^\varepsilon)(t_a) := \int_{t_a-\tau/2}^{t_a+\tau/2} K_\tau(s-t_a)\,\partial_s\mathbf{m}^\varepsilon(s)\,ds. \tag{3.5}$$

In practice we choose $\tau = O(\varepsilon)$ and therefore the computational cost of solving the micro model (3.4) is independent of the small scale parameter ε. Nevertheless, the theory and the method itself are not restricted by this assumption. Note that the initial data of the micro problem is given by the coarse scale solutions. This is necessary for synchronising the micro-problem with the current macroscopic quantities. Moreover, the macro stepsize is chosen larger than the size of the microscopic simulation box, i.e., $\tau < \triangle t$, so that the overall cost of the multiscale method is cheaper than the cost of a direct numerical approximation of the full multiscale problem.

Remark 3. *We emphasize that for computation of the flux (3.5), the micro problem must be solved forward and backward locally in time.*

The micro model does not include the damping term. This does not cause any big change in the dynamics of the macro-scale variable $\mathbf{M}$ owing to the fact that the solution $\mathbf{m}^\varepsilon$ of the micro model (3.4) with or without damping would precess around the field $\mathbf{H}^\varepsilon$ in both cases and the high frequency variations are filtered out in the upscaling step (3.5). It is possible to include the damping term in the micro problem but this requires removing the damping in the macroscopic model (3.2). It is also possible to carry out the local averaging in the upscaling (3.5) locally forward in time instead, i.e., in the interval $[0, \tau]$. Such a procedure will result in a qualitatively similar macroscopic solution but may lead to a significant deterioration in the order of convergence. The main advantage with using the conservative micro model (3.4) is that the nonlinearity is treated only in the macroscopic equation (3.2) which leads to significant simplifications in relation with the convergence analysis for the upscaling step and the numerical computation of the micro solution. Note that the macro-solver is also nonlinear, in $\mathbf{M}_{n+1}$, due to our choice of discretisation.

Remark 4. *The micro problem (3.4) can be posed instead over the domain $(0, \tau/2]$ by shifting the argument of the field $\mathbf{H}^\varepsilon$ by t_a:*

$$\begin{aligned} &\partial_t \mathbf{m}^\varepsilon(t) = \beta \mathbf{m}^\varepsilon(t) \times \mathbf{H}^\varepsilon(t + t_a), \quad t \in \tilde{I}_\tau^{\pm} \\ &\mathbf{m}^\varepsilon(0) = \mathbf{M}, \end{aligned} \tag{3.6}$$

where $\tilde{I}_\tau^+ := (0, \tau/2]$ and $\tilde{I}_\tau^- := (-\tau/2, 0]$. Accordingly, the flux (3.5) can be rewritten as

$$\mathbf{F}(t_a, \mathbf{M}) = \left(\mathcal{K}\partial_t \mathbf{m}^\varepsilon\right)(0) := \int_{-\tau/2}^{\tau/2} K_\tau(s)\, \partial_s \mathbf{m}^\varepsilon(s)\, ds. \tag{3.7}$$

3.3. **Modification for the stochastic microscale model.** In this case the microscopic magnetisation is driven by an external field which includes a random term, $\mathbf{H}^\varepsilon(t;\omega) := \mathbf{H}_0(t) + \mathbf{H}_1^\varepsilon(t;\omega)$, where $\mathbf{H}_1^\varepsilon(t;\omega)$ is a white noise with zero correlation in time. In practice, it has a zero mean but the method is not restricted by this assumption. Moreover, the macroscopic variables do not see these fluctuations. Therefore the macro model is deterministic and remains unchanged as in (3.2). The micro model is also the same as (3.4) but $\mathbf{H}^\varepsilon(t)$ is replaced by $\mathbf{H}^\varepsilon(t;\omega)$. The only fundamental modification appears in the upscaling step which now reads as

$$\text{Upscaling: } \mathbf{F}(t_a, M) = \left(\mathcal{K}\partial_t E[\mathbf{m}^\varepsilon]\right)(t_a) := \int_{t_a-\tau/2}^{t_a+\tau/2} K_\tau(s - t_a)\, \partial_s E[\mathbf{m}^\varepsilon(s;\omega)]\, ds.$$

In practice, the expectation $E[\mathbf{m}^\varepsilon]$ can be approximated by solving the micro problem for n different realisations and computing the average

$$E[\mathbf{m}^\varepsilon] \approx \frac{1}{n}\sum_{j=1}^{n} \mathbf{m}^\varepsilon(t,\omega_j).$$

In principle, due to ergodicity, one could avoid computing the expectation by instead solving the micro problem for a much larger larger τ. However, this should be avoided owing to computational inefficiency. As different realisations are embarrassingly parallel, the computational time of computing the expectation remains the same as that of the corresponding deterministic model if the computations are done in parallel.

Remark 5. *The HMM approach presented here is similar to the Landau-Lifshitz-Bloch models introduced in [22, 8] in the sense that all these approaches approximate the expected value of* $\mathbf{m}^\varepsilon$*. The LLB derived by Garanin, [22], works well for low temperatures but does not predict the right behaviour for elevated temperatures as the macroscopic magnetisation does not respect the power law at intermediate temperatures below the Curie temperature. Another strategy was suggested later in [8] to overcome this issue. The idea was to force the LLB, by properly fitting a parameter in the equation, so that the macroscopic magnetisation obeys the power law. At this stage, we are not able to make a further comparison between our HMM and the LLB type models. This is because to be able to see the temperature dependence of the average macroscopic magnetisation, an extension of the HMM to the general case with local averaging in time and space is needed. This is a work in progress. However, we emphasise here that when adapted to both the spatial and the temporal averaging setting, the HMM approach would potentially be more general than the LLB type macroscopic models which heavily rely on the classical molecular field approximation (MFA). This is due to the fact that with HMM it will be possible to upscale average quantities even in the presence of microscopic defects where MFA breaks down.*

4. Analysis

Without loss of generality we assume that $\beta = 1$. The LL equation with $\beta = 1$ can be written as

$$\partial_t \mathbf{m}^\varepsilon(t) = \mathcal{H}^\varepsilon(t)\mathbf{m}^\varepsilon(t) - \gamma \mathbf{m}^\varepsilon(t) \times (\mathcal{H}^\varepsilon(t)\mathbf{m}^\varepsilon(t)), \tag{4.1}$$

where $\mathcal{H}^\varepsilon(t) \in \mathbb{R}^{3\times 3}$ for all $t \in [0,T]$ is a skew-symmetric matrix function given by

$$\mathcal{H}^\varepsilon(t) = \begin{bmatrix} 0 & H_3^\varepsilon(t) & -H_2^\varepsilon(t) \\ -H_3^\varepsilon(t) & 0 & H_1^\varepsilon(t) \\ H_2^\varepsilon(t) & -H_1^\varepsilon(t) & 0 \end{bmatrix}.$$

For the analysis, we assume that $\mathcal{H}^\varepsilon(t) = \mathcal{H}(t, t/\varepsilon)$, where the field $\mathcal{H}(t,\cdot)$ is 1-periodic. By periodicity we can write

$$\mathcal{H}^\varepsilon(t+t_a) = \mathcal{H}(t+t_a, t/\varepsilon + r), \text{ where } r = \{t_a/\varepsilon\},$$

and $\{z\}$ represents the fractional part of z. To simplify the notation, we will write $\mathcal{H}_{t_a,r}(t,t/\varepsilon) := \mathcal{H}(t+t_a, t/\varepsilon + r)$. We assume that for all $\mathbf{v} \in \mathbb{R}^3$, and $k = 0, 1$, the following bounds hold

$$\left|\partial_t^k \mathcal{H}_{t_a.r}(t,z)\mathbf{v}\right|_2 \le c_1 \left|\mathbf{v}\right|_2, \quad \forall t \in [0,T] \text{ and } z \in \mathbb{R}. \tag{4.2}$$

In practice, in the ODE setting, it is often the case that $\mathcal{H}(t, t/\varepsilon) = \mathcal{H}_0 + \mathcal{H}_1(t/\varepsilon)$ where $\mathcal{H}_0$ is constant and hence $\partial_t \mathcal{H}(t, z) = 0$. However, we will keep the assumptions as above so that they are suitable also for more general cases when the solution $\mathbf{m}^\varepsilon$ might have a non-trivial dependence on the slow and fast temporal scales such as in the full PDE setting.

From the classical theory of averaging for oscillatory ODEs, see e.g. [10, 29], it follows that, when $\mathcal{H}(t, \cdot)$ is 1-periodic, the exact average magnetisation, $\bar{\mathbf{m}}$, is driven by the effective Hamiltonian $\bar{\mathcal{H}}(t) := \int_0^1 \mathcal{H}(t, s)\, ds$ and the effective equation reads as

$$\partial_t \bar{\mathbf{m}}(t) = \bar{\mathcal{H}}(t)\bar{\mathbf{m}}(t) - \gamma \bar{\mathbf{m}}(t) \times \left(\bar{\mathcal{H}}(t)\bar{\mathbf{m}}(t)\right), \quad \bar{\mathbf{m}}(0) = \mathbf{m}^\varepsilon(0). \tag{4.3}$$

Our aim in the next section is to show that the HMM solution $\mathbf{M}$ in (3.2) approximates the solution $\bar{\mathbf{m}}$ of the effective equation (4.3) without assuming any knowledge about the effective Hamiltonian $\bar{\mathcal{H}}$. The equation (4.3) is needed only for the analysis and the HMM does not use it.

Remark 6. *In what follows, we assume that the initial magnetisation $|\mathbf{M}_0|_2 = 1$. Figure 5.6 shows that the HMM introduces an error at later times and therefore the magnetisation length is not preserved exactly. See Remark 8 where we give an upper bound for this error, in the deterministic setting.*

4.1. **Upscaling error.** Our main result in this section is the following theorem which shows that the upscaling step in the HMM strategy captures the right macroscopic quantity.

Theorem 1. *Let $\bar{\mathcal{H}}(t) := \int_0^1 \mathcal{H}(t, s)ds$. Suppose that $\mathbf{m}^\varepsilon(t)$ solves the micro problem (3.6). Moreover, suppose that the assumptions (4.2) hold. Then $\mathbf{F}(t_a, \mathbf{M})$ given by the upscaling step (3.7) satisfies*

$$\left|\mathbf{F}(t_a, \mathbf{M}) - \bar{\mathcal{H}}(t_a)\mathbf{M}\right|_2 \leq C_1 \left(\tau + \left(\frac{\varepsilon}{\tau}\right)^{q+2}\right) |\mathbf{M}|_2 ,$$

where C_1 is independent of ε, and τ but may depend on p, q or K.

Proof. We start by rescaling $\mathbf{m}^\varepsilon$ to bring the $O(\varepsilon)$ oscillations back to $O(1)$ time scales. For this we introduce the fast time scale $\zeta = t/\varepsilon$

$$\mathbf{m}(\zeta; \varepsilon) := \mathbf{m}^\varepsilon(t).$$

Then we see that from (4.1)

$$\partial_t \mathbf{m}(t; \varepsilon) = \varepsilon \mathcal{H}_{t_a, r}(\varepsilon t, t)\mathbf{m}(t; \varepsilon). \tag{4.4}$$

We now Taylor expand $\mathbf{m}(t; \varepsilon)$ in terms of ε

$$\mathbf{m}(t; \varepsilon) = \mathbf{m}_0(t) + \varepsilon \mathbf{m}_1(t) + \frac{\varepsilon^2}{2}\mathbf{m}_2(t) + \cdots ,$$

where $\mathbf{m}_j(t) := \partial_\varepsilon^j \mathbf{m}(t; \varepsilon)|_{\varepsilon=0}$. From (4.4) and the definition of $\mathbf{m}_j$ with $j = 0$, we see that

$$\partial_t \mathbf{m}_0(t) = \partial_t \mathbf{m}(t; 0) = 0, \text{ and } \mathbf{m}_0(0) = \mathbf{m}^\varepsilon(0) = \mathbf{M}. \tag{4.5}$$

Hence $\mathbf{m}_0(t) = \mathbf{M}$. Moreover, for $j = 1$, we differentiate (4.4) with respect to ε and find that

$$\begin{aligned}\partial_t\partial_\varepsilon \mathbf{m}(t;\varepsilon) &= \partial_\varepsilon \left(\varepsilon \mathcal{H}_{t_a,r}\left(\varepsilon t, t\right)\mathbf{m}\left(t;\varepsilon\right)\right)\\ &= \mathcal{H}_{t_a,r}(\varepsilon t,t)\mathbf{m}(t;\varepsilon) + \varepsilon t \mathcal{H}^{(1)}_{t_a,r}(\varepsilon t,t)\mathbf{m}(t;\varepsilon) + \varepsilon \mathcal{H}_{t_a,r}(\varepsilon t,t)\partial_\varepsilon \mathbf{m}(t;\varepsilon),\end{aligned}$$

where $\mathcal{H}^{(k)}_{t_a,r}(t,z) := \partial_t^k \mathcal{H}_{t_a,r}(t,z)$. Upon putting $\varepsilon = 0$, we obtain

$$\partial_t \mathbf{m}_1(t) = \mathcal{H}_{t_a,r}(0,t)\mathbf{m}_0(t), \quad \mathbf{m}_1(0) = 0. \tag{4.6}$$

We now define $\mathbf{e}_{tail}(t;\varepsilon) := \mathbf{m}(t;\varepsilon) - (\mathbf{m}_0(t) + \varepsilon \mathbf{m}_1(t))$. We can then write

$$\begin{aligned}\partial_t \mathbf{m}^\varepsilon(t) &= \partial_t \left(\mathbf{m}_0(t/\varepsilon) + \varepsilon \mathbf{m}_1(t/\varepsilon)\right) + \partial_t \mathbf{e}_{tail}(t/\varepsilon;\varepsilon)\\ &= \partial_\zeta \mathbf{m}_1(t/\varepsilon) + \partial_t \mathbf{e}_{tail}(t/\varepsilon;\varepsilon) = \mathcal{H}_{t_a,r}(0,t/\varepsilon)\mathbf{m}_0(t/\varepsilon) + \partial_t \mathbf{e}_{tail}(t/\varepsilon;\varepsilon)\\ &= \mathcal{H}_{t_a,r}(0,t/\varepsilon)\mathbf{M} + \partial_t \mathbf{e}_{tail}(t/\varepsilon;\varepsilon).\end{aligned}$$

From the last equality, it follows that

$$\begin{aligned}\left|\mathbf{F}(t_a,\mathbf{M}) - \bar{\mathcal{H}}(t_a)\mathbf{M}\right|_2 &:= \left|\int_{-\tau/2}^{\tau/2} K_\tau\left(s\right)\partial_s \mathbf{m}^\varepsilon(s)\, ds - \bar{\mathcal{H}}(t_a)\mathbf{M}\right|_2\\ &= \left|\int_{-\tau/2}^{\tau/2} K_\tau\left(s\right)\mathcal{H}_{t_a,r}(0,s/\varepsilon)\mathbf{M}\, ds + \int_{-\tau/2}^{\tau/2} K_\tau\left(s\right)\partial_s \mathbf{e}_{tail}(s/\varepsilon;\varepsilon)\, ds - \bar{\mathcal{H}}(t_a)\mathbf{M}\right|_2\\ &\le \underbrace{\left|\int_{-\tau/2}^{\tau/2} K_\tau\left(s\right)\mathcal{H}_{t_a,r}(0,s/\varepsilon)\, ds\mathbf{M} - \bar{\mathcal{H}}(t_a)\mathbf{M}\right|_2}_{E_{averaging}} + \underbrace{\left|\int_{-\tau/2}^{\tau/2} K_\tau\left(s\right)\partial_s \mathbf{e}_{tail}(s/\varepsilon;\varepsilon)\, ds\right|_2}_{E_{tail}}\end{aligned}$$

By Lemma 1, we have $E_{averaging} \le C\left(\frac{\varepsilon}{\tau}\right)^{q+2}|\mathbf{M}|_2$. Moreover, by Lemma 3 presented below, it follows that $E_{tail} \le C\tau\,|\mathbf{M}|_2$. The proof is completed. □

4.2. **The tail error.** The following lemma quantifies the tail error that arises from replacing $\mathbf{m}$ by $\tilde{\mathbf{m}} := \mathbf{m}_0 + \varepsilon\mathbf{m}_1$, where $\mathbf{m}_0$ and $\mathbf{m}_1$ are given in (4.5) and (4.6) respectively, in the upscaling step.

Lemma 3. *Suppose that the assumptions (4.2) hold and that*

$$\tilde{\mathbf{m}}(t;\varepsilon) := \mathbf{m}_0(t) + \varepsilon\mathbf{m}_1(t), \quad \text{and} \quad \mathbf{e}(t;\varepsilon) := \mathbf{m}(t;\varepsilon) - \tilde{\mathbf{m}}(t;\varepsilon),$$

where $\mathbf{m}_0$ and $\mathbf{m}_1$ are given in (4.5) and (4.6), respectively. Moreover, let $K \in \mathbb{K}^{p,q}$ and $\tau \ge \varepsilon$. Then

$$\left|\int_{-\tau/2}^{\tau/2} K_\tau(t)\partial_t \mathbf{e}(t/\varepsilon;\varepsilon)\, dt\right| \le C\tau\,|\mathbf{M}|_2\,, \tag{4.7}$$

where C is independent of ε, τ and T but may depend on $\mathcal{H}_{t_a,r}$.

Proof. By definition we can write, with $\delta\mathcal{H}_{t_a,r} := \mathcal{H}_{t_a,r}(\varepsilon t,t) - \mathcal{H}_{t_a,r}(0,t)$,

$$\begin{aligned}\partial_t \mathbf{e}(t;\varepsilon) &= \partial_t \mathbf{m}(t;\varepsilon) - \partial_t \tilde{\mathbf{m}}(t;\varepsilon) = \partial_t \mathbf{m}(t;\varepsilon) - \varepsilon\partial_t \mathbf{m}_1(t)\\ &= \varepsilon\mathcal{H}_{t_a,r}(\varepsilon t,t)\mathbf{m}(t;\varepsilon) - \varepsilon\mathcal{H}_{t_a,r}(0,t)\mathbf{m}_0(t)\\ &= \varepsilon\mathcal{H}_{t_a,r}(\varepsilon t,t)\mathbf{e}(t;\varepsilon) + \varepsilon\mathcal{H}_{t_a,r}(\varepsilon t,t)\tilde{\mathbf{m}}(t;\varepsilon) - \varepsilon\mathcal{H}_{t_a,r}(0,t)\mathbf{m}_0(t)\\ &= \varepsilon\mathcal{H}_{t_a,r}(\varepsilon t,t)\mathbf{e}(t;\varepsilon) + \varepsilon\delta\mathcal{H}_{t_a,r}\mathbf{m}_0(t) + \varepsilon^2\mathcal{H}_{t_a,r}(\varepsilon t,t)\mathbf{m}_1(t).\end{aligned}$$

Moreover, taking the inner-product of the above equation with $\mathbf{e}$ we get

$$\begin{aligned}\langle \partial_t \mathbf{e}, \mathbf{e}\rangle &= \varepsilon\langle \mathcal{H}_{t_a,r}(\varepsilon t, t)\mathbf{e}, \mathbf{e}\rangle + \varepsilon\langle \delta\mathcal{H}_{t_a,r}\mathbf{m}_0(t), \mathbf{e}\rangle + \varepsilon^2\langle \mathcal{H}_{t_a,r}(\varepsilon t, t)\mathbf{m}_1(t), \mathbf{e}\rangle \\ &= \varepsilon\langle \delta\mathcal{H}_{t_a,r}\mathbf{m}_0(t), \mathbf{e}\rangle + \varepsilon^2\langle \mathcal{H}_{t_a,r}(\varepsilon t, t)\mathbf{m}_1(t), \mathbf{e}\rangle.\end{aligned}$$

This implies the inequality

$$\frac{1}{2}\partial_t \left|\mathbf{e}(t;\varepsilon)\right|_2^2 \le \left(\varepsilon \left|\delta\mathcal{H}_{t_a,r}\mathbf{m}_0(t)\right|_2 + \varepsilon^2 \left|\mathcal{H}_{t_a,r}(\varepsilon t, t)\mathbf{m}_1(t)\right|_2\right) \left|\mathbf{e}(t;\varepsilon)\right|_2. \tag{4.8}$$

By the assumptions (4.2) and a Taylor's expansion, we have $\left|\delta\mathcal{H}_{t_a,r}\mathbf{m}_0\right|_2 \approx \varepsilon t \left|\mathbf{M}\right|_2$. For the second term, we again use (4.2) and (4.6). This gives

$$\begin{aligned}\left|\mathcal{H}_{t_a,r}(\varepsilon t, t)\mathbf{m}_1(t)\right|_2 \le C\left|\mathbf{m}_1(t)\right|_2 &= C\left|\int_0^t \mathcal{H}(0,s)\mathbf{m}_0\, ds\right|_2 \\ &\le C\int_0^t \left|\mathcal{H}(0,s)\mathbf{m}_0\right|_2\, ds \le Ct\left|\mathbf{M}\right|_2.\end{aligned}$$

An application of inequality (2.2) in Lemma 2 for (4.8) yields

$$\left|\mathbf{e}(t;\varepsilon)\right|_2 \le \int_0^t \varepsilon\left|\delta\mathcal{H}_{t_a,r}\mathbf{m}_0(s)\right|_2 + \varepsilon^2\left|\mathcal{H}_{t_a,r}(\varepsilon s, s)\mathbf{m}_1(s)\right|_2\, ds \le C\varepsilon^2\left(1+t^2\right)\left|\mathbf{M}\right|_2. \tag{4.9}$$

We can now bound the tail error in the upscaling procedure. With $\alpha := \varepsilon/\tau$, we have

$$\begin{aligned}\left(\mathcal{K}\partial_t\mathbf{e}(t/\varepsilon;\varepsilon)\right)(0) &:= \int_{-\tau/2}^{\tau/2} K_\tau(t)\partial_t\mathbf{e}(t/\varepsilon;\varepsilon)\, dt = \frac{1}{\tau}\int_{-\tau/2}^{\tau/2} K(t/\tau)\partial_t\mathbf{e}(t/\varepsilon;\varepsilon)\, dt \\ &= -\frac{1}{\tau}\int_{-\tau/2}^{\tau/2}\frac{1}{\tau}K'(t/\tau)\mathbf{e}(t/\varepsilon;\varepsilon)\, dt = -\alpha\int_{-1/2\alpha}^{1/2\alpha}\frac{1}{\tau}K'(t\alpha)\mathbf{e}(t;\varepsilon)\, dt.\end{aligned}$$

Finally, we use (4.9) to obtain

$$\left|\left(\mathcal{K}\partial_t\mathbf{e}(t/\varepsilon;\varepsilon)\right)(0)\right| \le \left|K'\right|_\infty \frac{1}{\tau}\max_{t\in[-\frac{1}{2\alpha},\frac{1}{2\alpha}]}\left|\mathbf{e}(t;\varepsilon)\right|_2 \le C\tau\left|\mathbf{M}\right|_2.$$

□

4.3. **Estimates for the full solution.** In this section, we give a fully discrete error estimate for the difference between the HMM solution given in (3.3) and the solution of the exact locally-averaged equation (4.3). For this, let us denote the HMM solution by $\{\mathbf{M}_n^{\triangle t,\delta t}\}_{n=0}^N$. This is the solution that is computed by solving the micro and the macro problems in a discrete setting. We define also a semi-discrete solution $\{\mathbf{M}_n^{\triangle t}\}_{n=0}^N$ which is essentially the HMM solution but when the micro problem is solved exactly. Moreover, we introduce $\{\bar{\mathbf{m}}_j^{\triangle t}\}_{j=1}^N$ which approximates the solution of the effective equation (4.3) by the implicit midpoint rule:

$$\bar{\mathbf{m}}_{n+1}^{\triangle t} = \bar{\mathbf{m}}_{n+1}^{\triangle t} + \triangle t\bar{\mathcal{H}}(t_{n+1/2})\bar{\mathbf{m}}_{n+1/2}^{\triangle t} + \mathbf{N}_\gamma[\bar{\mathbf{m}}_{n+1/2}^{\triangle t}], \quad \bar{\mathbf{m}}_0^{\triangle t} = \mathbf{m}^\varepsilon(0), \tag{4.10}$$

where $\bar{\mathbf{m}}_{n+1/2} := \frac{1}{2}\left(\bar{\mathbf{m}}_{n+1} + \bar{\mathbf{m}}_n\right)$ and

$$\mathbf{N}_\gamma[\bar{\mathbf{m}}_{n+1/2}^{\triangle t}] := -\gamma\bar{\mathbf{m}}_{n+1/2}^{\triangle t} \times \left(\bar{\mathcal{H}}(t_{n+1/2})\bar{\mathbf{m}}_{n+1/2}^{\triangle t}\right).$$

On the other hand, we see from equation (3.3) that the HMM solution satisfies

(4.11)
$$\begin{aligned}\mathbf{M}_{n+1}^{\triangle t} &= \mathbf{M}_n^{\triangle t} + \triangle t \mathbf{F}(t_{n+1/2}, \mathbf{M}_{n+1/2}^{\triangle t}) - \gamma \triangle t \mathbf{M}_{n+1/2}^{\triangle t} \times \mathbf{F}(t_{n+1/2}, \mathbf{M}_{n+1/2}^{\triangle t}) \\ &= \mathbf{M}_n^{\triangle t} + \triangle t \left(\bar{\mathcal{H}}(t_{n+1/2}) \mathbf{M}_{n+1/2}^{\triangle t} + E_{n+1/2}^{ups} \right) + \triangle t \mathbf{N}_\gamma[\mathbf{M}_{n+1/2}^{\triangle t}] \\ &\quad - \gamma \triangle t \mathbf{M}_{n+1/2}^{\triangle t} \times E_{n+1/2}^{ups},\end{aligned}$$

where $E_{n+1/2}^{ups} := \mathbf{F}(t_{n+1/2}, \mathbf{M}_{n+1/2}) - \bar{\mathcal{H}}(t_{n+1/2}) \mathbf{M}_{n+1/2}$ satisfies the estimate in Theorem 1. We can then split the overall error into three parts as follows

$$\left| \mathbf{M}_n^{\triangle t, \delta t} - \bar{\mathbf{m}}(t_n) \right|_2 \leq \underbrace{\left| \mathbf{M}_n^{\triangle t, \delta t} - \mathbf{M}_n^{\triangle t} \right|_2}_{E_{micro}} + \underbrace{\left| \mathbf{M}_n^{\triangle t} - \bar{\mathbf{m}}_n^{\triangle t} \right|_2}_{E_{HMM}} + \underbrace{\left| \bar{\mathbf{m}}_n^{\triangle t} - \bar{\mathbf{m}}(t_n) \right|_2}_{E_{Macro}}.$$

The first and the last errors are the micro and the macro discretisation errors, which can be bounded in a rather standard way. The HMM error E_{HMM} is, however, related to the upscaling error E_n^{ups} which was estimated in Theorem 1. In what follows we will firstly prove a theorem which provides an upper-bound for the error E_{HMM} for the case $\gamma = 0$.

Theorem 2. *Suppose that $\{\mathbf{M}_n^{\triangle t}\}_{n=0}^N$ solves (3.3) with $\beta = 1$ and $\gamma = 0$, where the associated micro problem (3.4) is solved exactly. Moreover, assume $K \in \mathbb{K}^{p,q}$ and that $\bar{\mathbf{m}}_{n+1}^{\triangle t}$ solves 4.10 and $\triangle t \leq 2/3$. Then the error $\mathbf{e}_n^{\triangle t} := \mathbf{M}_n^{\triangle t} - \bar{\mathbf{m}}_n^{\triangle t}$ satisfies*

$$|\mathbf{e}_N^{\triangle t}|_2 \leq C\sqrt{T} \left(\tau + \left(\frac{\varepsilon}{\tau} \right)^{q+2} \right) \max_{0 \leq n \leq N} |\mathbf{M}_{n+1/2}^{\triangle t}|_2,$$

where $T = N \triangle t$, and C is a constant independent of ε, τ and T but may depend on $\mathcal{H}, p, q, K$.

Proof. For simplicity we drop $\triangle t$ in the notation and instead write $\mathbf{e}_n$. We can see, from (4.10) and (4.11), that

$$\mathbf{e}_{n+1} = \mathbf{e}_n + \triangle t \bar{\mathcal{H}}(t_{n+1/2}) \mathbf{e}_{n+1/2} + \triangle t E_{n+1/2}^{ups}, \quad \mathbf{e}_0 = 0.$$

Next we rearrange the above scheme and take the inner-product with $\mathbf{e}_{n+1/2}$. This gives

$$\begin{aligned}\langle \mathbf{e}_{n+1} - \mathbf{e}_n, \mathbf{e}_{n+1/2} \rangle &= \triangle t \langle \bar{\mathcal{H}}(t_{n+1/2}) \mathbf{e}_{n+1/2}, \mathbf{e}_{n+1/2} \rangle + \triangle t \langle E_{n+1/2}^{ups}, \mathbf{e}_{n+1/2} \rangle \\ &= \triangle t \langle E_{n+1/2}^{ups}, \mathbf{e}_{n+1/2} \rangle.\end{aligned}$$

We now use the relation $\mathbf{e}_{n+1/2} = \frac{1}{2}(\mathbf{e}_{n+1} + \mathbf{e}_n)$ and write

$$\langle \mathbf{e}_{n+1} - \mathbf{e}_n, \frac{1}{2}(\mathbf{e}_{n+1} + \mathbf{e}_n) \rangle = \frac{1}{2} \langle \mathbf{e}_{n+1}, \mathbf{e}_{n+1} \rangle - \frac{1}{2} \langle \mathbf{e}_n, \mathbf{e}_n \rangle = \triangle t \langle E_{n+1/2}^{ups}, \mathbf{e}_{n+1/2} \rangle.$$

From here and the fact that $\mathbf{e}_0 = 0$, it follows that

$$\begin{aligned}\langle \mathbf{e}_N, \mathbf{e}_N\rangle &= \sum_{n=0}^{N-1} \left(\langle \mathbf{e}_{n+1}, \mathbf{e}_{n+1}\rangle - \langle \mathbf{e}_n, \mathbf{e}_n\rangle\right) = 2\triangle t \sum_{n=0}^{N-1} \langle E^{ups}_{n+1/2}, \mathbf{e}_{n+1/2}\rangle \\ &\leq \triangle t \sum_{n=0}^{N-1} \left|E^{ups}_{n+1/2}\right|^2 + \triangle t \sum_{n=0}^{N-1} \left|\mathbf{e}_{n+1/2}\right|^2 \\ &\leq \triangle t \sum_{n=0}^{N-1} \left|E^{ups}_{n+1/2}\right|^2 + \triangle t \sum_{n=0}^{N-1} |\mathbf{e}_n|^2 + \frac{\triangle t}{2} |\mathbf{e}_N|^2 .\end{aligned}$$

We have with $\triangle t \leq 2/3$,

$$\begin{aligned}|\mathbf{e}_N|^2 &\leq \left(1 - \frac{\triangle t}{2}\right)^{-1} \left(N\triangle t \max_{0\leq n\leq N-1} \left|E^{ups}_{n+1/2}\right|_2^2 + \triangle t \sum_{n=0}^{N-1} |\mathbf{e}_n|^2\right) \\ &\leq \left(1 - \frac{\triangle t}{2}\right)^{-1} N\triangle t \max_{0\leq n\leq N-1} \left|E^{ups}_{n+1/2}\right|_2^2 + \frac{2\triangle t}{2-\triangle t} \sum_{n=0}^{N-1} |\mathbf{e}_n|^2 \\ &\leq \frac{3}{2} N\triangle t \max_{0\leq n\leq N-1} \left|E^{ups}_{n+1/2}\right|_2^2 + \sum_{n=0}^{N-1} |\mathbf{e}_n|^2 .\end{aligned}$$

By a simple induction and an application of Theorem 1 we obtain

$$E_{HMM} := \left|\mathbf{M}_N^{\triangle t} - \bar{\mathbf{m}}_N^{\triangle t}\right|_2 \leq C\sqrt{T}\left(\tau + \left(\frac{\varepsilon}{\tau}\right)^{q+2}\right).$$

□

Remark 7. *Note the constraint on the time step, $\triangle t \leq 2/3$, in Theorem 2. It appears despite using the implicit midpoint rule on the macro level. Nevertheless, the restriction on the time step does not influence the efficiency as it still allows for large macroscopic stepsizes.*

We present now a lemma which estimates the length of the macroscopic magnetisation at different discrete time instants.

Lemma 4. *Suppose that $\{\mathbf{M}_n^{\triangle t}\}_{n=0}^N$ solves (4.11) with an initial magnetisation that satisfies $|\mathbf{M}_0|_2 = 1$. Moreover, let $K \in \mathbb{K}^{p,q}$ and $\delta = \tau + (\varepsilon/\tau)^{q+2}$. Then*

$$|\mathbf{M}_n|_2 \leq \exp(Ct_n \frac{\delta}{1 - \frac{\delta\triangle t}{2}}) = 1 + O(\delta),$$

where C is a constant independent of n, ε, τ and $t_n = n\triangle t$.

Proof. We take the inner-product of (4.11) with $\mathbf{M}_{n+1/2}$. Following the same idea as in the proof of Theorem 2 and using Theorem 1 we obtain

$$\begin{aligned}\langle \mathbf{M}_{n+1} - \mathbf{M}_{n+1}\rangle - \langle \mathbf{M}_n - \mathbf{M}_n\rangle &= 2\triangle t \langle E^{ups}_{n+1/2}, \mathbf{M}_{n+1/2}\rangle \\ &\leq \triangle t |E^{ups}_{n+1/2}|_2 |\mathbf{M}_{n+1/2}|_2 \leq C\triangle t\delta |\mathbf{M}_{n+1/2}|_2^2 \\ &\leq C\frac{\triangle t\delta}{2}\left(|\mathbf{M}_{n+1}|_2^2 + |\mathbf{M}_n|_2^2\right).\end{aligned}$$

Hence

$$|\mathbf{M}_{n+1}|_2^2 \leq \left(\frac{1 + C\frac{\delta\triangle t}{2}}{1 - C\frac{\delta\triangle t}{2}}\right) |\mathbf{M}_n|_2^2.$$

From here and the fact that $|\mathbf{M}_0|_2 = 1$ it follows that, with $z := x/(1-x)$ where $x = C\frac{\delta\triangle t}{2}$,

$$|\mathbf{M}_n|_2^2 \leq \left(\frac{1 + C\frac{\delta\triangle t}{2}}{1 - C\frac{\delta\triangle t}{2}}\right)^n = (1+2z)^n \leq \exp(2nz).$$

The final result follows by putting $t_n = n\triangle t$. □

We now present a theorem where an estimate of the HMM error, E_{HMM}, for the nonlinear case when $\gamma > 0$ is given.

Theorem 3. *Suppose that $\{\mathbf{M}_n^{\triangle t}\}_{n=0}^N$ solves (3.3) with $\beta = 1$ and $\gamma > 0$, where the associated micro problem (3.4) is solved exactly. Moreover, assume $K \in \mathbb{K}^{p,q}$ and that $\bar{\mathbf{m}}_{n+1}^{\triangle t}$ solves (4.10) and $\triangle t \leq \frac{2}{3(1+2c_1\gamma+2C_1\gamma)}$, where $C_1 = O(1)$ is a constant such that $|\mathbf{M}_{n+1/2}^{\triangle t}|_2 \leq C_1$, and*

$$\langle \partial_{\mathbf{M}}\mathbf{N}_\gamma(\bar{\mathbf{m}}_{n+1/2} + \theta\mathbf{e}_{n+1/2})\mathbf{e}_{n+1/2}, \mathbf{e}_{n+1/2}\rangle \leq \gamma c_1 \left|\mathbf{e}_{n+1/2}\right|_2^2, \quad \forall \quad \theta \in [0,1].$$

Then the error $\mathbf{e}_n^{\triangle t} = \mathbf{M}_n^{\triangle t} - \bar{\mathbf{m}}_n^{\triangle t}$ satisfies

$$\left|\mathbf{e}_N^{\triangle t}\right|_2 \leq C\sqrt{T}\left(\tau + \left(\frac{\varepsilon}{\tau}\right)^{q+2}\right) \max_{0\leq n\leq N}\left|\mathbf{M}_{n+1/2}^{\triangle t}\right|_2,$$

where $T = N\triangle t$, and C is a constant independent of ε, τ and T but may depend on $\mathcal{H}, p, q, K$ or γ.

Proof. For convenience we write $-\gamma\mathcal{J}$ to denote the Jacobian $\partial_{\mathbf{M}}\mathbf{N}_\gamma$ and we remove $\triangle t$ in the notations. By (4.10) and (4.11), we see that the error $\mathbf{e}_n$ satisfies

$$\begin{aligned}
\mathbf{e}_{n+1} &= \mathbf{e}_n + \triangle t\bar{\mathcal{H}}(t_{n+1/2})\mathbf{e}_{n+1/2} + \triangle t E_{n+1/2}^{ups} + \triangle t\left(\mathbf{N}_\gamma[\mathbf{M}_{n+1/2}] - \mathbf{N}_\gamma[\bar{\mathbf{m}}_{n+1/2}]\right) \\
&\quad - \gamma\triangle t\mathbf{M}_{n+1/2} \times E_{n+1/2}^{ups} \\
&= \mathbf{e}_n + \triangle t\bar{\mathcal{H}}(t_{n+1/2})\mathbf{e}_{n+1/2} + \triangle t E_{n+1/2}^{ups} - \gamma\triangle t\mathcal{J}[\bar{\mathbf{m}}_{n+1/2} + \theta\mathbf{e}_{n+1/2}]\mathbf{e}_{n+1/2} \\
&\quad - \gamma\triangle t\mathbf{M}_{n+1/2} \times E_{n+1/2}^{ups}.
\end{aligned}$$

Hence

$$\begin{aligned}
\langle \mathbf{e}_{n+1} - \mathbf{e}_n, \mathbf{e}_{n+1}\rangle &= \triangle t\langle E_{n+1/2}^{ups}, \mathbf{e}_{n+1/2}\rangle - \gamma\triangle t\langle \mathcal{J}[\bar{\mathbf{m}}_{n+1/2} + \theta\mathbf{e}_{n+1/2}]\mathbf{e}_{n+1/2}, \mathbf{e}_{n+1/2}\rangle \\
&\quad - \gamma\triangle t\langle \mathbf{M}_{n+1/2} \times E_{n+1/2}^{ups}, \mathbf{e}_{n+1/2}\rangle.
\end{aligned}$$

We now use the fact that by Lemma 4 $|\mathbf{M}_{n+1/2}|_2 \leq C_1$, where $C_1 = O(1)$ for sufficiently small values for δ and we proceed similar to the analysis of the linear

case. Moreover, we define $\kappa := (1 + 2c_1\gamma + 2C_1\gamma)$ and find that

$$\begin{aligned}
\langle \mathbf{e}_N, \mathbf{e}_N\rangle &= \sum_{n=0}^{N-1} \left(\langle \mathbf{e}_{n+1}, \mathbf{e}_{n+1}\rangle - \langle \mathbf{e}_n, \mathbf{e}_n\rangle\right) \\
&= 2\triangle t \sum_{n=0}^{N-1} \langle E^{ups}_{n+1/2}, \mathbf{e}_{n+1/2}\rangle - 2\gamma\triangle t \sum_{n=0}^{N-1} \langle \mathcal{J}[\bar{\mathbf{m}}_{n+1/2} + \theta \mathbf{e}_{n+1/2}]\mathbf{e}_{n+1/2}, \mathbf{e}_{n+1/2}\rangle \\
&- 2\gamma\triangle t \sum_{n=0}^{N-1} \langle \mathbf{M}_{n+1/2} \times E^{ups}_{n+1/2}, \mathbf{e}_{n+1/2}\rangle \\
&\leq \triangle t \sum_{n=0}^{N-1} \left|E^{ups}_{n+1/2}\right|^2 + (1 + 2c_1\gamma)\triangle t \sum_{n=0}^{N-1} \left|\mathbf{e}_{n+1/2}\right|^2 + 2C_1\gamma\triangle t \sum_{n=0}^{N-1} \left|E^{ups}_{n+1/2}\right|^2 \\
&\quad + \left|\mathbf{e}_{n+1/2}\right|^2 \leq (1 + 2C_1\gamma)\triangle t \sum_{n=0}^{N-1} \left|E^{ups}_{n+1/2}\right|^2 + \kappa\triangle t \sum_{n=0}^{N-1} |\mathbf{e}_n|^2 + \kappa\frac{\triangle t}{2} |\mathbf{e}_N|^2 .
\end{aligned}$$

Now let $\triangle t \leq \frac{2}{3\kappa}$. Then

$$\begin{aligned}
|\mathbf{e}_N|_2^2 &\leq \frac{1 + 2C_1\gamma}{1 - \kappa\triangle t/2} N\triangle t \max_{0\leq n\leq N} \left|E^{ups}_{n+1/2}\right|^2 + \sum_{n=0}^{N-1} |\mathbf{e}_n|^2 \\
&\leq \frac{3\kappa}{2} T \max_{0\leq n\leq N} \left|E^{ups}_{n+1/2}\right|^2 + \sum_{n=0}^{N-1} |\mathbf{e}_n|^2 .
\end{aligned}$$

A simple induction together with an application of Theorem 1 yields the desired estimate. □

Remark 8. *Using the error estimates in Theorems 2 and 3, the estimate in Lemma 4 and the fact that* $|\bar{\mathbf{m}}_n^{\triangle t}|_2 = 1$*, one can see that*

$$\begin{aligned}
\left||\mathbf{M}_N^{\triangle t,\delta t}|_2 - 1\right| &\leq \left|\mathbf{M}_N^{\triangle t,\delta t} - \mathbf{M}_N^{\triangle t}\right| + \left|\bar{\mathbf{m}}_N^{\triangle t} - \mathbf{M}_N^{\triangle t}\right| + \Big|\underbrace{\left|\bar{\mathbf{m}}_N^{\triangle t}\right|}_{=1} - 1\Big| \\
&\leq E_{micro} + C\sqrt{T}\left(\tau + \left(\frac{\varepsilon}{\tau}\right)^{q+2}\right),
\end{aligned}$$

which shows that the magnetisation length does not remain constant for HMM type multiscale couplings but that the error can be reduced down to $O(\varepsilon)$ *by using high order methods at the micro level and by choosing* $\tau \approx \varepsilon^{1-\beta}$*, for* $\beta = 1/(q+2)$*.*

5. Numerical results

5.1. **The tail error.** In this section, we aim at illustrating the validity of the expansion made in the proof of Theorem 1. For this we solve the problem (4.4) between $0 \leq t \leq 1$ with the initial condition $\mathbf{M} = [0, 0, 1]^T$, and the external field

$$\mathbf{H}(t, z) = [0, 0, 1]^T + [\sin(2\pi z), \cos(2\pi z), 0]^T.$$

We study the convergence for two cases: (i) The convergence against $\mathbf{m}_0$, where $\mathbf{m}_0 = \mathbf{M}$, (ii) The convergence against the truncated solution $\tilde{\mathbf{m}}(t;\varepsilon) = \mathbf{m}_0 + \varepsilon\mathbf{m}_1(t)$, where $\mathbf{m}_1$ solves (4.6). The error is defined as

$$E_{tail} = \max_{0\le t\le 1} |\mathbf{m}(t;\varepsilon) - \mathbf{u}(t;\varepsilon)|_2\,, \qquad \text{where } \mathbf{u}(t;\varepsilon) = \mathbf{m}_0 \text{ or } \tilde{\mathbf{m}}(t;\varepsilon).$$

The left plot in Figure 5.1 shows that we gain one order in ε upon including the term $\mathbf{m}_1$ in the expansion and, in particular, that the estimate (4.7) holds.

5.2. **The upscaling error.** We show now evidence that the estimate, for the upscaling error, given in Theorem 1, is sharp. For this we compare the upscaled flux in (3.5) with the exact effective flux $\bar{\mathcal{H}}(t)\mathbf{M}$ for $\mathbf{M} = [0,0,1]^T$. The micro problem is solved with the initial data $[0,0,1]^T$ and the external field

$$\mathbf{H}^\varepsilon(t) = [0,0,1]^T + [\cos(2\pi t/\varepsilon), \cos(2\pi t/\varepsilon), 0]^T. \tag{5.1}$$

In this case $\bar{\mathcal{H}} = [0,0,1]^T$. The convergence is shown for two cases: (i) By setting $\tau = 5.3\varepsilon$, and letting $\varepsilon \longrightarrow 0$ for increasing values of q, where higher q means a better regularity for the kernel K, see the right plot in Figure 5.1 (ii) By fixing $\tau = 0.1$ and $\tau = 0.2$ and study the difference as $\varepsilon \longrightarrow 0$, see the Figure 5.2. Both tests corroborate our theoretical findings in Theorem 1.

5.3. **The full solution.** In Figure 5.3, we consider two examples with

$$\mathbf{H}(t, t/\varepsilon) = \mathbf{H}_0 + \mathbf{H}_1(t/\varepsilon),$$

where $\mathbf{H}_1(t) = [\sin(2\pi t), \cos(2\pi t), 0]^T$ or $\mathbf{H}_1(t) = [\sin(2\pi t)^2, \cos(2\pi t)^2, 0]^T$ and $\mathbf{H}_0 = [0,0,1]^T$ in both cases. We observe that, in the former, the solution $\mathbf{m}^\varepsilon$ converges to $[0,0,1]^T$ as T increases whereas in the latter, the solution converges to a non-trivial limit given by the average. In both cases, the HMM solution captures the coarse features of the exact solution using only 20 discretisation points.

Moreover, in Figure 5.4 we provide the results for external fields with a random term

$$\mathbf{H}(t, t/\varepsilon) = \mathbf{H}_0 + \mathbf{H}^\varepsilon_{sto}, \quad \mathbf{H}^\varepsilon_{sto} = \mathbf{H}_1(t/\varepsilon) + \mathbf{H}_2(t;\omega) \tag{5.2}$$

where $\mathbf{H}_1(t) = [\sin(2\pi t), \cos(2\pi t), 0]^T$, $\mathbf{H}_2\,dt = \sqrt{\sigma}\,d\mathbf{W}(t)$, with $\mathbf{W}(t)$ a Wiener-process and where the measure is interpreted in the Stratonovich sense, and $\sigma = 0.0001$. In the left plot we compare the HMM solution computed by only one realisation in the upscaling with $E[\mathbf{m}^\varepsilon]$, whereas in the right plot we compare the HMM solution computed by 20 realisations in the upscaling step against $E[\mathbf{m}^\varepsilon]$. This figure shows the need for computing the expected value in the upscaling step. All other parameters in the simulation are stated in the description of Figure 5.4. Note that in these simulations, i.e., Figures 5.3 and 5.4, we considered the high damping scenario by choosing $\gamma = 1$. Moreover, to illustrate the performance of the method for a low damping parameter, we take $\gamma = 0.1$ and we see that the coarse scale features are again captured nicely for the deterministic and the stochastic high frequency fields, see Figure 5.5. Note that, in Figure 5.5 all parameters other than γ is chosen exactly in the same manner as in Figure 5.3 for the deterministic and as in Figure 5.4 for the stochastic settings.

5.4. **Magnetisation amplitude.** We consider the full problem with an external field of the form (5.1), where $\mathbf{H}_1(t) = [\sin(2\pi t), \cos(2\pi t), 0]^T$ and $\mathbf{H}_0 = [0, 0, 1]^T$ and we look at two scenarios: (i) For a fixed ε we keep track of the evolution of the magnetisation amplitude over the macro time steps, (ii) We study the deviation of the magnetisation amplitude in comparison to the initial length of magnetisation as we refine the small scale parameter ε. The initial magnetisation is given as $\mathbf{M}_0 = \frac{1}{\sqrt{3}}[1, 1, 1]^T$ so that $|\mathbf{M}_0| = 1$. Figure 5.6 shows that the HMM does not preserve the initial length of the magnetisation. In the left plot, we show the evolution of the magnetisation amplitude for each macroscopic time when $\varepsilon = 0.01$. In this simulation we have used $N\triangle t = 2\pi$ and $N = 20$. The magnetisation length $|\mathbf{M}_n|$ for $n > 0$ clearly deviates from $|\mathbf{M}_0| = 1$. In the right plot, however, we study the convergence

$$\max_{0\leq n\leq N} ||\mathbf{M}_n|_2 - |\mathbf{M}_0|_2| \longrightarrow 0$$

as $\varepsilon \longrightarrow 0$, for $N\triangle t = 1$ and $N = 10$. The simulation result verifies the expected convergence rate stated in Remark 8. In the simulations we have chosen a kernel $K \in \mathbb{K}^{p,q}$ with $p = 1$ and $q = 7$. Moreover, we set $\tau = 5.3\varepsilon$ and observe $O(\varepsilon)$ convergence in the selected range of ε. Note that the $O((\varepsilon/\tau)^{q+2})$ error term is not seen in this simulation since we have used a large q.

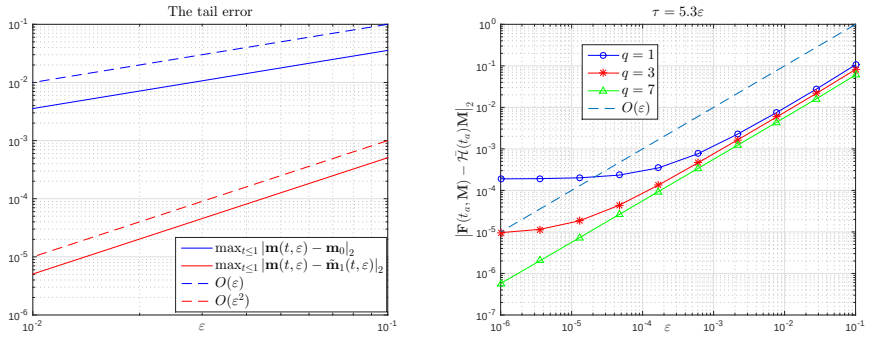

FIGURE 5.1. (Left) The differences $\mathbf{m} - \mathbf{m}_0$ and $\mathbf{m} - \tilde{\mathbf{m}}$, where $\tilde{\mathbf{m}} = \mathbf{m}_0 + \varepsilon\mathbf{m}_1$ as $\varepsilon \longrightarrow 0$ are shown. The result shows that the estimate (4.7) is sharp. (Right) The upscaling error, which is estimated in Theorem 1, is depicted. An averaging domain of size $\tau = 5.3\varepsilon$ is used in the simulation. The constant part of the error corresponds to $O((\varepsilon/\tau)^{q+2})$ from Theorem 1 and it decreases upon using smoother kernels with high q. This result confirms the error estimate from the Theorem.

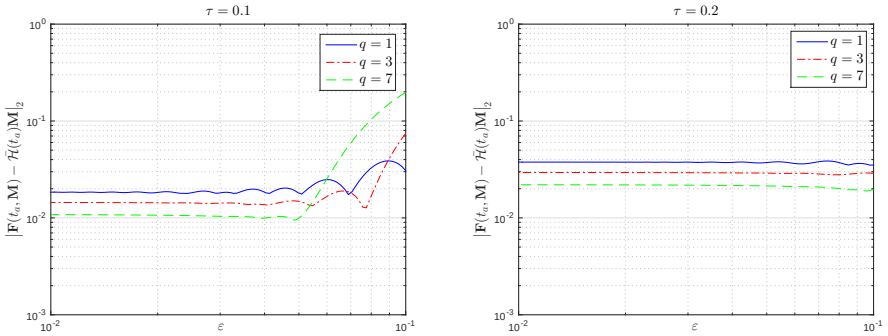

FIGURE 5.2. The upscaling error from Theorem 1 is shown. The error, $|\mathbf{F} - \bar{\mathcal{H}}(t_a)\mathbf{M}|_2$, as $\varepsilon \longrightarrow 0$ is depicted for (Left) $\tau = 0.1$, (Right) $\tau = 0.2$. The results verify the estimate in the theorem.

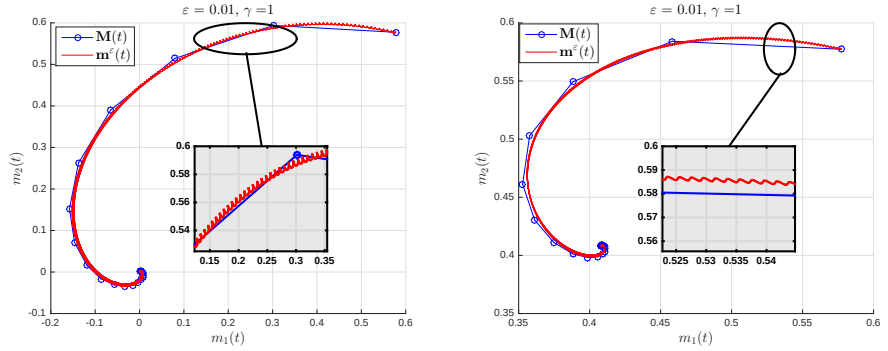

FIGURE 5.3. The HMM solution $\mathbf{M}$ with $\mathbf{H}(t, t/\varepsilon) = \mathbf{H}_0 + \mathbf{H}_1(t/\varepsilon)$, where $\mathbf{H}_0 = [0, 0, 1]^T$ and (Left) $\mathbf{H}_1(t/\varepsilon) = [\sin(2\pi t/\varepsilon), \cos(2\pi t/\varepsilon), 0]^T$ (Right) $\mathbf{H}_1(t/\varepsilon) = [\sin(2\pi t/\varepsilon)^2, \cos(2\pi t/\varepsilon)^2, 0]^T$, for $\varepsilon = 0.01$ is compared to the exact solution $\mathbf{m}^\varepsilon$. We have used $\beta = 1$, $\gamma = 1$, $\tau = 5\varepsilon$, $T = 2\pi$, $\triangle t = T/20$ and a kernel $K \in \mathbb{K}^{p,q}$ with $p = 5, q = 4$ in the simulations. The average behaviour of the fine scale solution is recovered by using only 20 points on the macroscopic grid.

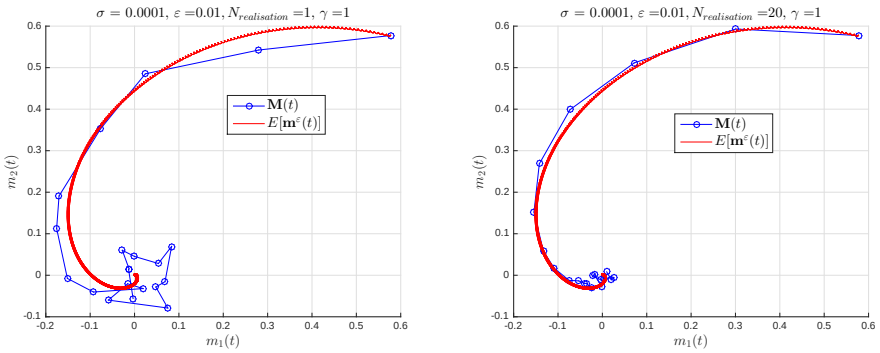

FIGURE 5.4. The HMM solution $\mathbf{M}$ with $\mathbf{H}(t, t/\varepsilon) = \mathbf{H}_0 + \mathbf{H}^\varepsilon_{sto}$, where $\mathbf{H}^\varepsilon_{sto}$ is given in (5.2) with $\sigma = 0.0001$. The paremeters $\beta, \gamma, T, \triangle t$ and K are chosen as in Figure 5.3 and $\varepsilon = 0.0033, \tau = 15\varepsilon$ is used in this simulation. (Left) The HMM solution with only one realisation in the upscaling step is compared to $E[\mathbf{m}^\varepsilon]$ (Right) The HMM solution with 20 realisations in the upscaling step is compared to $E[\mathbf{m}^\varepsilon]$. The average behaviour of the fine scale solution is recovered by using only 20 points on the macroscopic grid.

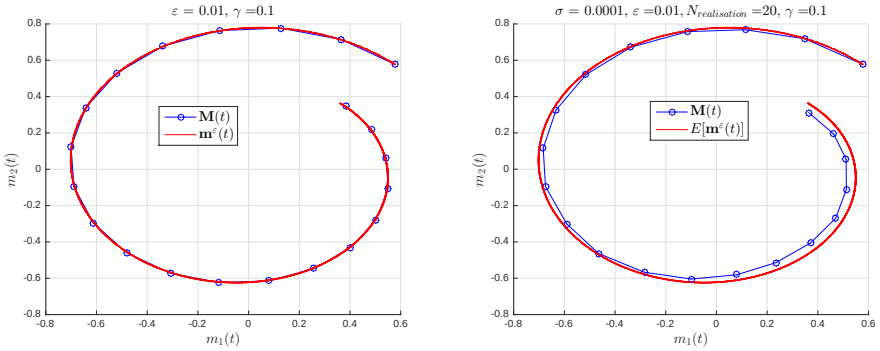

FIGURE 5.5. The HMM solution $\mathbf{M}$ with (Left) $\mathbf{H}^\varepsilon = \mathbf{H}_0 + \mathbf{H}_1(t/\varepsilon)$, where $\mathbf{H}_0 = [0, 0, 1]^T$ and $\mathbf{H}_1(t/\varepsilon) = [\sin(2\pi t/\varepsilon), \cos(2\pi t/\varepsilon), 0]^T$ (Right) $\mathbf{H}^\varepsilon = \mathbf{H}_0 + \mathbf{H}^\varepsilon_{sto}$, where $\mathbf{H}_0 = [0, 0, 1]^T$ and $\mathbf{H}^\varepsilon_{sto}$ is given in (5.2) with $\sigma = 0.0001$. We have used $\beta = 1, \gamma = 0.1, \tau = 5\varepsilon, T = 2\pi, \triangle t = T/20$ and a kernel $K \in \mathbb{K}^{p,q}$ with $p = 5, q = 4$ in the simulations. The average behaviour of the fine scale solution is recovered by using only 20 points on the macroscopic grid.

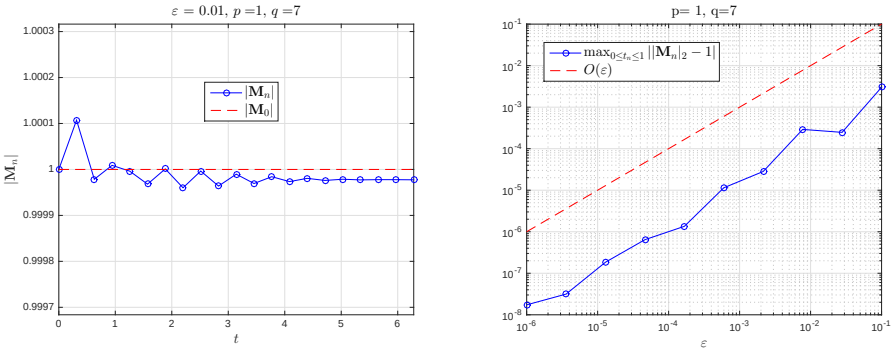

FIGURE 5.6. The magnetisation amplitude $|\mathbf{M}_n|_{n=0}^N$ with $H(t, t/\varepsilon) = \mathbf{H}_0 + \mathbf{H}_1(t/\varepsilon)$, where $\mathbf{H}_0 = [0, 0, 1]^T$ and $\mathbf{H}_1(t) = [\sin(2\pi t), \cos(2\pi t), 0]^T$ is computed using a kernel $K \in \mathbb{K}^{p,q}$ with $p = 1$ and $q = 7$. (Left) The evolution of the magnetisation amplitude is illustrated for $\varepsilon = 0.01$. The HMM does not conserve the initial length. (Right) The convergence of the magnetisation length to unit length, as $\varepsilon \longrightarrow 0$, for $\tau = 5.3\varepsilon$ is depicted. The $O(\varepsilon)$ convergence rate is in a good agreement with the estimate provided in Remark 8. The error $O((\varepsilon/\tau)^{q+2})$ is not seen in this plot as q is chosen sufficiently large.

6. Discussion

We have proposed and analysed a multiscale method based on the HMM framework for coupling disparate time scales in the Landau-Lifshitz equations of micromagnetism. The current study serves as a first step in designing general upscaling algorithms for incorporating effects of microscopic variations into smoothly varying macroscopic dynamics.

As a model problem we have considered a simple case where the microscopic model is driven by a high frequency field. We have shown that the HMM captures the right effective quantities by proving an error estimate between the HMM and the exact averaged dynamics. Two important outcomes of the analysis are: (i) The error between the HMM and the exact dynamics consist of discretisation errors in the micro and macro levels and the upscaling error which can be pushed down to $O(\varepsilon)$, where $\varepsilon \ll 1$ is a typical lengthscale representing the ratio between the fine and the coarse scales, (ii) Unlike one-scale methods such as the implicit midpoint rule, the multiscale algorithms would, in general, suffer from non-constant length of the magnetisation. However this error can be controlled upon choosing an appropriate high-order micro solver along with a suitable choice for the size of the local averaging domain, see Remark 8. Alternatively, a projection step could be added at each time iteration to project the magnetisation to the unit sphere, which is a common practice in micro-magnetic simulations, see e.g. [20, 27]. Moreover, the proposed microscopic and macroscopic models can be easily used with any time-stepping scheme.

We believe that the results in the present article give a good insight regarding the nature of the errors that may appear in more general settings where the effective field contains influences of spatial variations as well. The proposed method can potentially be used to approximate macroscopic effects that may arise in different physical problems such as spin waves. The extension of the current method to problems in micro-magnetism with multiple scales in spatial and temporal dimensions is under investigation and will be addressed in upcoming reports.

References

[1] A. Abdulle, W. E, B. Engquist, and E. Vanden-Eijnden, *The heterogeneous multiscale method*, Acta Numerica, 21 (2012), pp. 1–87.

[2] A. Aharoni, *Mathematical theory of ferromagnetism*, Oxford Un. Press, 1996.

[3] G. Ariel, B. Engquist, S. J. Jim, and R. Tsai, *Iterated averaging of three-scale oscillatory systems*, Commun. Math. Sci., 12 (2014), pp. 791–824.

[4] G. Ariel, B. Engquist, and R. Tsai, *Numerical multiscale methods for coupled oscillators*, Multiscale Model. Sim., 7 (2009), pp. 1387–1404.

[5] G. Ariel, B. Engquist, and R. Tsai, *A reversible multiscale integration method*, Comm. Math. Sci., 7 (2009), pp. 595–610.

[6] D. Arjmand and O. Runborg, *Analysis of heterogeneous multiscale methods for long time wave propagation problems*, Multiscale Model. Sim., 12 (2014), pp. 1135–1166.

[7] D. Arjmand and O. Runborg, *A time dependent approach for removing the cell boundary error in elliptic homogenization problems*, to appear in J. Comp. Phys., (2016), doi:10.1016/j.jcp.2016.03.009.

[8] L. Banas, Z. Brzezniak, M. Neklyudov, and A. Prohl, *Stochastic ferromagnetism*, De Gruyter Studies in Mathematics 58, 2014.

[9] L. Banas, A. Prohl, and M. Slodicka, *Numerical scheme for augmented landau-lifshitz equation in heat assisted recording*, J. Comput. Appl. Math., 236 (2012), pp. 4775–4787.
[10] N. N. Bogoliubov and Y. A. Mitropolski, *Asymptotic methods in the theory of non-linear oscillations*, New York: Gordon and Breach, 1961.
[11] W. F. Brown, *Thermal fluctuations of a single-domain particle*, Phys. Rev., 130 (1963), pp. 1677–1686.
[12] F. Bruckner, C. Vogler, B. Bergmair, T. Huber, M. Fuger, D. Suess, M. Feischl, T. Fuehrer, M. Page, and D. Praetorius, *Combining micromagnetism and magnetostatic maxwell equations for multi-scale magnetic simulations*, J. Magn. Magn. Mat., 343 (2013), pp. 163–168.
[13] J. Chen, C. J. Garcia-Cervera, and X. Yang, *A mean-field model for spin dynamics in mutilayered ferromagnetic media*, Multiscale Model. Sim., 13 (2015), pp. 551–570.
[14] I. Cimrak, *A survey on the numerics and computations for the landau-lifshitz equation of micromagnetism*, Arch. Comp. Meth. Eng., 15 (2008), pp. 277–309.
[15] M. d'Aquino, C. Serpico, and G. Miano, *Geometrical integration of landau-lifshitz-gilbert equation based on the mid-point rule*, J. Comp. Phys., 209 (2005), pp. 730–753.
[16] V. Dobrovitski, M. Katnelson, and B. Harmon, *Statistical coarsegraining as an approach to multiscale problems in magnetism*, J. Magn. Magn. Mat., 221 (2000), pp. L235–L242.
[17] W. E, *Analysis of the heterogeneous multiscale method for ordinary differential equations*, Commun. Math. Sci., 1 (2003), pp. 423–436.
[18] W. E and B. Engquist, *The heterogeneous multiscale methods*, Commun. Math. Sci., 1 (2003), pp. 87–133.
[19] W. E, D. Liu, and E. Vanden-Eijnden, *Analysis of multiscale methods for stochastic differential equations*, Commun. on Pure and Appl. Math., LVIII (2005), pp. 1544–1585.
[20] W. E and X. P. Wang, *Numerical methods for the landau-lifshitz equation*, SIAM J. Numer. Anal., 38 (2000), pp. 1647–1665.
[21] B. Engquist and R. Tsai, *Heterogeneous multiscale methods for stiff ordinary differential equations*, Math. Comp., 74 (2005), pp. 1707–1742.
[22] D. A. Garanin, *Fokker-planck and landau-lifshitz-bloch equations for classical ferromagnets*, Phys. Rev. B, 55 (1997).
[23] G. Grinstein and R. H. Koch, *Coarse graining in micromagnetics*, Phys. Rev. Lett., 90 (2003), pp. 207201–1–4.
[24] C. Kittel, *On the theory of ferromagnetic resonance absorption*, Phys. Rev., 73 (1948), pp. 155–161.
[25] M. Kruzik and A. Prohl, *Recent developments in the modeling, analysis, and numerics of ferromagnetism*, SIAM Rev., 48 (2006), pp. 439–483.
[26] L. Landau and E. Lifshits, *On the theory of the dispersion of magnetic permeability in ferromagnetic bodies*, Phys. Zeitsch. der Sow., 8 (1935), pp. 153–169.
[27] D. Lewis and N. Nigam, *Geometric integration on spheres and some interesting applications*, J. Comp. Appl. Math., 151 (2003), pp. 141–170.
[28] R. I. McLachlan, K. Modin, and O. Verdier, *Symplectic integrators for spin systems*, Phys. Rev. E, 89 (2014).

[29] G. A. Pavliotis and A. Stuart, *Multiscale methods: Averaging and homogenization*, Text in Applied Mathematics, Springer, 2008.
[30] M. Poluektov, O. Eriksson, and G. Kreiss, *Scale transitions in magnetisation dynamics*, 2015. Preprint.
[31] A. Prohl, *Computational micromagnetism*, Advances in Numerical Mathematics, 2001.
[32] W. Scholz, T. Schrefl, and J. Fidler, *Micromagnetic simulation of thermally activated switching in fine particles*, J. Magn. Magn. Mat., 233 (2001), pp. 296–304.
[33] V. Tsiantos, W. Scholz, D. Suess, T. Schrefl, and J. Fidler, *The effect of the cell size in langevin micromagnetic simulations*, J. Magn. Magn. Mat., 242–245 (2002), pp. 999–1001.
[34] E. Vanden-Eijnden, *Numerical techniques for multiscale dynamical systems with stochastic effects*, Commun. Math. Sci., 1 (2003), pp. 385–391.

E-mail address: doghonay.arjmand, stefane, gunilla.kreiss@it.uu.se

Division of Scientific Computing, Department of Information Technology, Uppsala University, SE-751 05 Uppsala, Sweden.